

1-aminocyclopropane-1-carboxylic acid signals independently of ethylene in the FEI cellulose synthesis pathway in *Arabidopsis thaliana*

Abstract

Cellulose is an important structural molecule in the plant cell wall. Recently, the receptor-like kinases FEI1 and FEI2 were found to regulate cellulose synthesis. When grown on high sucrose media, the *feilfei2* double mutant has short, swollen roots due to cellulose deficiency. The phytohormone ethylene is known to inhibit root elongation, thus causing root growth defects. The *feilfei2* phenotype is not reverted to wild-type when ethylene perception is disrupted, indicating that ethylene is not involved in the FEI pathway. However, a reversion of the *feilfei2* phenotype has been observed when ethylene biosynthesis is inhibited. In the ethylene biosynthesis pathway, 1-aminocyclopropane-1-carboxylic acid (ACC) is the direct precursor to ethylene. This, together with other genetic and biochemical studies, suggests that ACC acts as a signal in the FEI pathway. We have found that the ethylene-insensitive line, *ein2-5*, responds to the application of ACC but not ethylene, suggesting that ACC signals independently of ethylene. Additionally, ACC reestablishes swelling in *feilfei2ein2-5* mutants in which ethylene biosynthesis has been inhibited. Here, we examined the role of ACC in cellulose biosynthesis to confirm the biochemical effects of ACC in the FEI pathway. To do so, we genetically and physiologically disrupted ethylene biosynthesis and signaling in a *feilfei2* background. Our findings on the role of ACC in the FEI signaling pathway and thus cellulose synthesis will likely impact industry, where understanding cell wall composition may lead to enhanced production of cellulose-based goods such as paper and biofuels.

Introduction

The plant cell wall consists of various polysaccharides, including the main load-bearing element, cellulose. Cellulose consists of β 1,4-linked glucose and is synthesized at the plasma membrane by hexamers of cellulose synthase complexes. The glucose chains crystallize to form cellulose microfibrils (Arioli et al. 1998). These microfibrils guide cell growth by organizing perpendicularly to the direction of growth. Most plant cells grow anisotropically—in a directionally dependent manner—due to microfibrils restricting radial expansion. When the cell wall is perturbed due to, for instance, disruption of the orientation of the cellulose microfibrils, cells grow isotropically—equally in all directions. This can result in root swelling, as seen in the roots of the *Arabidopsis sabre* mutant (Aeschbacher et al. 1995). Ethylene is known to mediate root growth defects and studies blocking ethylene perception and biosynthesis were performed on the *sabre* mutant. Interestingly, blocking ethylene biosynthesis with α -aminoisobutyric acid (AIB) or its perception with silver ions reverts the root swelling of the *sabre* mutant to wild-type morphology (Aeschbacher et al. 1995).

In plants, ethylene biosynthesis occurs through an enzyme-catalyzed pathway beginning with the conversion of methionine to *S*-adenosyl methionine (AdoMet) (**Fig. 1**). ACC synthase (ACS) converts AdoMet into 1-aminocyclopropane-1-carboxylic acid (ACC). Lastly, ACC is converted by ACC oxidase (ACO) into ethylene (Wang et al. 2002).

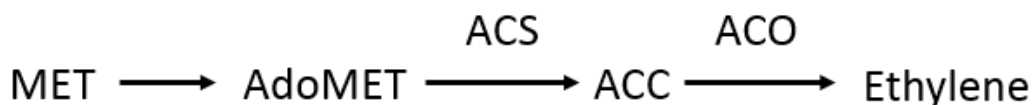


Figure 1. Ethylene is synthesized from methionine in an enzyme-catalyzed pathway. Methionine (MET) is converted to *S*-adenosylmethionine (AdoMET). AdoMET is converted to ACC by the ACC SYNTHASES (ACS). ACC is then converted to ethylene by the ACC OXIDASES (ACO).

Ethylene is perceived at the endoplasmic reticulum (ER) by the receptor, ETHYLENE RESPONSE 1 (ETR1) (**Fig. 2**). In the presence of ethylene, ETR1 inactivates CONSTITUTIVE TRIPLE RESPONSE 1 (CTR1), which cannot phosphorylate its downstream target ETHYLENE INSENSITIVE 2 (EIN2) in its inactive state. When not phosphorylated, the C-terminal end of EIN2 is cleaved and moves into the nucleus to regulate ethylene response genes (Ju et al. 2012). Additionally, the C-terminal end of EIN2 acts in the cytoplasm to translationally inhibit the degradation proteins, EIN3 BINDING F-BOX 1 and 2 (EBF1, EBF2) (Li et al. 2015).

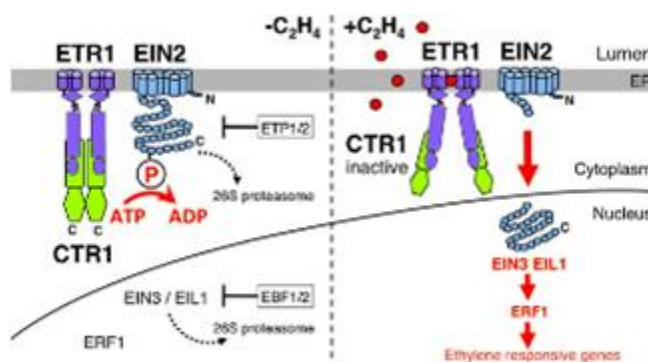


Figure 2. The ethylene signaling pathway in the absence (left) and presence (right) of ethylene. When ethylene is absent, CTR1 phosphorylates EIN2 which inhibits EIN2 C-terminal cleavage and prevents downstream signal transduction. In the presence of ethylene, ER-localized ETR1 inactivates CTR1, which allows the C-terminal end of EIN2 to be cleaved and move into the nucleus to regulate ethylene response genes (Ju et al. 2012).

In *Arabidopsis*, ACS proteins are encoded by the genes *ACS2,4,5,6,7,8,9*, and *11*, while the *ACO1,2,3,4,5* genes encode the ACO proteins (Givens 2010, Tsuchisaka et al. 2009). The ACS proteins are classified into three families based on variation of their C-terminal domain. Type-1 proteins include ACS1, 2, and 6; type-2 proteins include ACS4, 5, 8, 9, and 11; and type 3 proteins include ACS7. The type 1 proteins have a long C terminal end that contains a calcium-dependent protein kinase (CDPK) phosphorylation site and three mitogen-activated protein kinase (MAPK) phosphorylation sites, while the type 2 proteins have only the CDPK site, and

the type 3 proteins have no predicted phosphorylation sites. *ACS10* and *ACS12* are pseudogenes and *ACS1* forms a non-functional homodimer (Tsuchisaka et al. 2009).

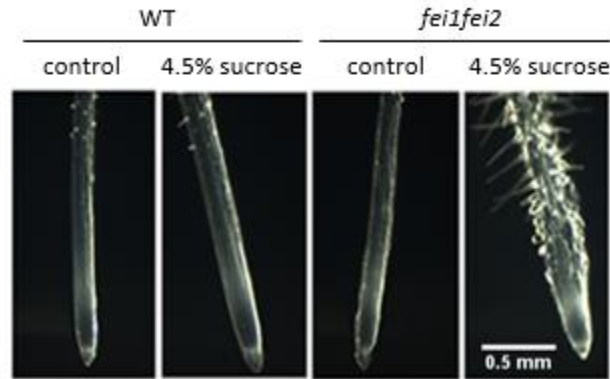


Figure 3. *fei1fei2* root swelling compared to the wild-type (wt) Columbia-0 (Col-0) plant. The *fei1fei2* mutant displays a swollen root phenotype on high sucrose, but not on low sucrose.

Cell wall integrity signaling is not well defined in plants, but these signaling mechanisms are important regulators of cell growth and expansion. This involves signaling for cell wall hydration, extension, wall crosslinking, and the deposition of new materials such as cellulose (Wolf et al. 2012). Two leucine rich repeat-receptor like kinases, FEI1 and FEI2, have been shown to regulate cellulose biosynthesis. The *fei1fei2* mutant displays a short, swollen root phenotype on high sucrose media due to lower levels of cellulose (**Fig. 3**) (Xu et al. 2008). Because of the phenotypic similarity to the *sabre* mutant, ethylene biosynthesis and perception was inhibited in the *fei1fei2* mutant to determine if ethylene was the signal acting in the FEI pathway as well. Ethylene biosynthesis was blocked using aminooxyacetic acid (AOA), a molecule that interferes with enzymes that require pyroxydial phosphate, and α -aminoisobutyric acid (AIB), a structural analog of ACC (Xu et al. 2008). Ethylene perception was inhibited using 1-methylcyclopropene (1-MCP) and silver thiosulfate, which act at the level of ethylene receptors. Ethylene signaling was disrupted genetically as well, using *ein2-50*, a null ethylene insensitive mutant, and *etr1*, a null ethylene receptor mutant. Surprisingly, only blocking

ethylene biosynthesis, but not ethylene perception, through either genetic or biochemical mechanisms, reverted the swelling of the *fei1fei2* roots (Xu et al. 2008). This suggested that an ACC-derived signal other than ethylene was acting in this pathway. Several additional pieces of evidence point towards ACC itself as this signaling molecule. For instance, similar to the reversion of the *fei* mutants, swelling in root tips caused by isoxaben, an herbicide that targets cellulose synthesis, was reverted by blocking ethylene biosynthesis but not ethylene perception (Tsang et al. 2011). Moreover, a study of the high order *acs* mutants (*acs2*, 4, 5, 6, 7, 9, *ami8*, *11*) showed that mutations in all eight of the functional *ACS* genes resulted in embryonic lethality (Tsuchisaka et al. 2009). This stands in contrast to ethylene-insensitive mutants that are completely viable (Guzman 1990).

Here, we tested the role of ACC in the FEI pathway in order to clarify its function as a signal during plant development. To determine if reducing ACC levels genetically will reduce swelling similarly to the AIB application, the CRISPR-Cas9 system was used to target the functional *ACS* genes. Because the type-2 *ACS* proteins interact with the FEI proteins in yeast-two hybrid assays (Xu et al. 2008), we hypothesized that a null type-2 *acs* mutant line might restore a wild-type phenotype in *fei1fei2* mutants. Additionally, a type-1 and -3 mutant line was crossed with a type-2 mutant line to confirm previous effects of an octuple *acs* mutant line (Tsuchisaka et al. 2009). We also designed CRISPR constructs to create a null *aco1,2,3,4,5* mutant to determine if inhibiting the conversion of ACC to ethylene will result in a build-up of ACC, and if this increase in ACC enhances the *fei* phenotype. These results help clarify the role of ACC as a signal in the FEI cellulose synthesis pathway and in plant development.

Results

Testing fei1fei2ein2-5 response to ACC and AIB

Previous experiments done by Xu et al. (2008) showed that *feilfei2* root swelling is reverted to wild-type root morphology when grown on media containing α -aminoisobutyric acid media. If AIB competes with ACC in the FEI signaling pathway, application of ACC might partially reestablish swelling when applied to roots along with AIB. However, ethylene is known to cause shortened root growth and ACC is often used as a substitution for ethylene in experiments. Thus, a *feilfei2ein2-5* mutant was created to inhibit ethylene signaling to confirm that the root morphology effects of ACC were not due to ethylene signaling. The swollen root phenotype is retained in the *feilfei2ein2-5* line when grown on 4.5% sucrose. When AIB is applied to the *feilfei2ein2-5* line, the root swelling was reverted to wild-type root morphology. When ACC was applied in conjunction with AIB, roots were shortened and swelling was restored (**Fig. 4C**). Interestingly, *ein2-5* is sensitive to ACC in these assays, and further experiments are being conducted to investigate the function of ACC in this context (**Fig. 4D**).

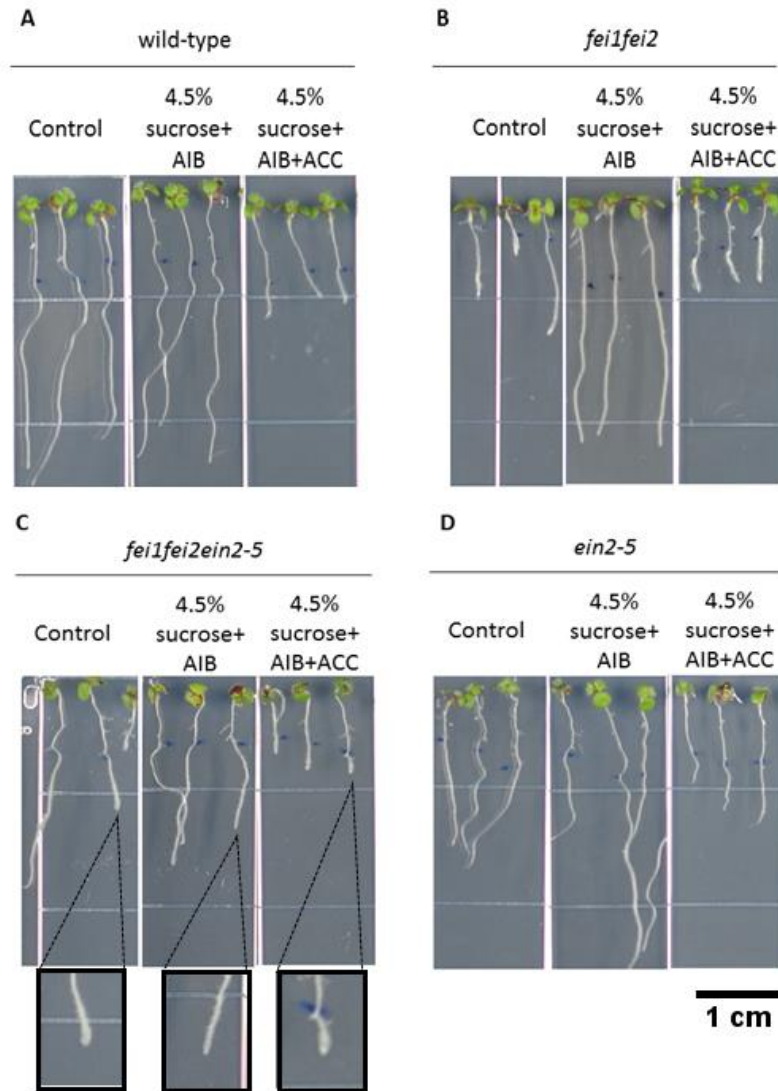


Figure 4. Swollen roots of *fei1fei2ein2-5* swelling is partially restored when grown on high sucrose media supplemented with 0.4mM AIB and 10uM ACC. **A.** WT roots do not swell on high sucrose. Roots are not affected by AIB, but display a short root when exposed to ACC. **B.** *fei1fei2* roots swell on high sucrose media. AIB application reverts swelling to wild-type morphology. ACC application reestablishes swelling. **C.** *fei1fei2ein2-5* roots swell on high sucrose media. AIB reverts swelling to wild-type morphology. ACC application reestablishes swelling. **D.** *ein2-5* roots do not swell on high sucrose media. Roots are not affected by AIB but display a short root when exposed to ACC.

Examining the effects of ACC on ein2-5 mutants

Because *ein2-5* surprisingly displayed sensitivity to ACC application, further experiments were conducted to confirm ethylene insensitivity of the *ein2-5* line. Wild-type and *ein2-5* seedlings were grown on ACC media or were flushed with ethylene. Wild-type plants display a short root in response to ethylene and ACC, and *ein2-5* seedlings only display a short root in response to ACC (**Fig. 5A**). Additionally, Street and Schaller replicated these results with more precise concentrations of ethylene (**Fig. 5B**). This data shows that *ein2-5* is sensitive to ACC but not ethylene and suggests that ACC signals independently of ethylene.

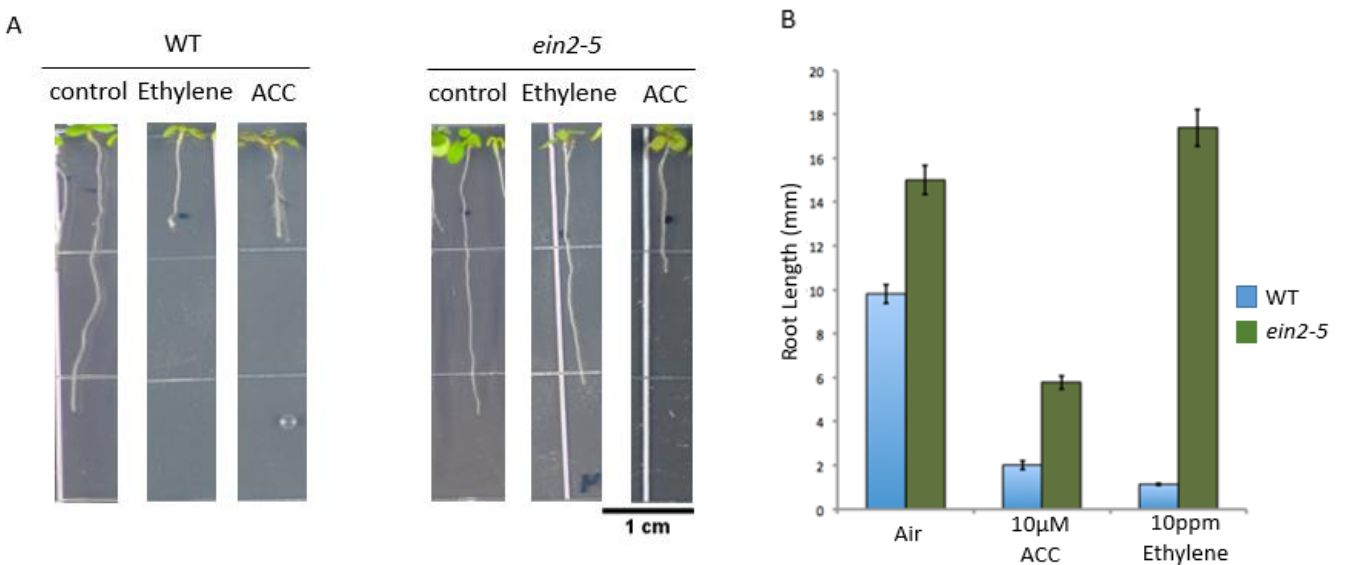


Figure 5. *ein2-5* roots are sensitive to ACC application but not ethylene, suggesting that ACC signals independently of ethylene. **A.** Wild-type and *ein2-5* seedlings were flushed with 10ppm ethylene or grown on 10μM ACC and imaged after four days. **B.** Quantification of roots (data from Street and Schaller, personal communication) shows that seedling roots are sensitive to ACC but not ethylene.

Creating acs and aco mutants using T-DNA insertions

To determine if genetic disruption of ACC signaling mimics the previous pharmacological experiments, I worked to generate an *acs4,5,8,9,11,fei1fei2* septuple mutant.

Initially, available T-DNA lines (Alonso et al. 2003) were used to create the high order *acs* mutant and a line homozygous for *feilfei2acs2,4,8,9,11* and heterozygous for *acs5* was obtained. However, plants genotyped for the *acs5* mutation always yielded a T-DNA heterozygosity and never segregated in the next generations, likely due to chromosomal rearrangements. Such rearrangements have been previously reported in both *Arabidopsis* and tobacco T-DNA studies (Nacry et al. 1998). Therefore, CRISPR/Cas9 technology has been implemented to target the *acs* genes.

If ACC OXIDASE function is inhibited, a build-up of ACC could occur due to an inability to convert ACC to ethylene. We aimed to determine if an increase in ACC exacerbated the *feilfei2* phenotype on both high and low sucrose by creating a null *feilfei2aco1,2,3,4,5* mutant. To create the *aco* mutant, I initially used the available *aco* T-DNA SALK lines in *ACO2,3* and *4* (Alonso et al. 2003). While the root width was not measured here, the swelling qualitatively did not appear to be more severe than *feilfei2* in the *feilfei2aco2,3,4* mutant. Additionally, there was no enhancement of the *fei* phenotype in the *feilfei2aco2,3,4* mutant when grown on low sucrose (**Fig. 6A**). There was no significant difference between the average root length of the *aco2,3,4feilfei2* mutants and the *feilfei2* mutants, indicating the *fei* phenotype is not enhanced in a triple *aco2,3,4* mutant (**Fig. 6B**). Because *ACO1* and *ACO5* are still functional, these gene products may have compensated for the loss of the other three *ACO* genes. Thus, CRISPR/Cas9 has been used to create a complete null line for all five *ACO* genes.

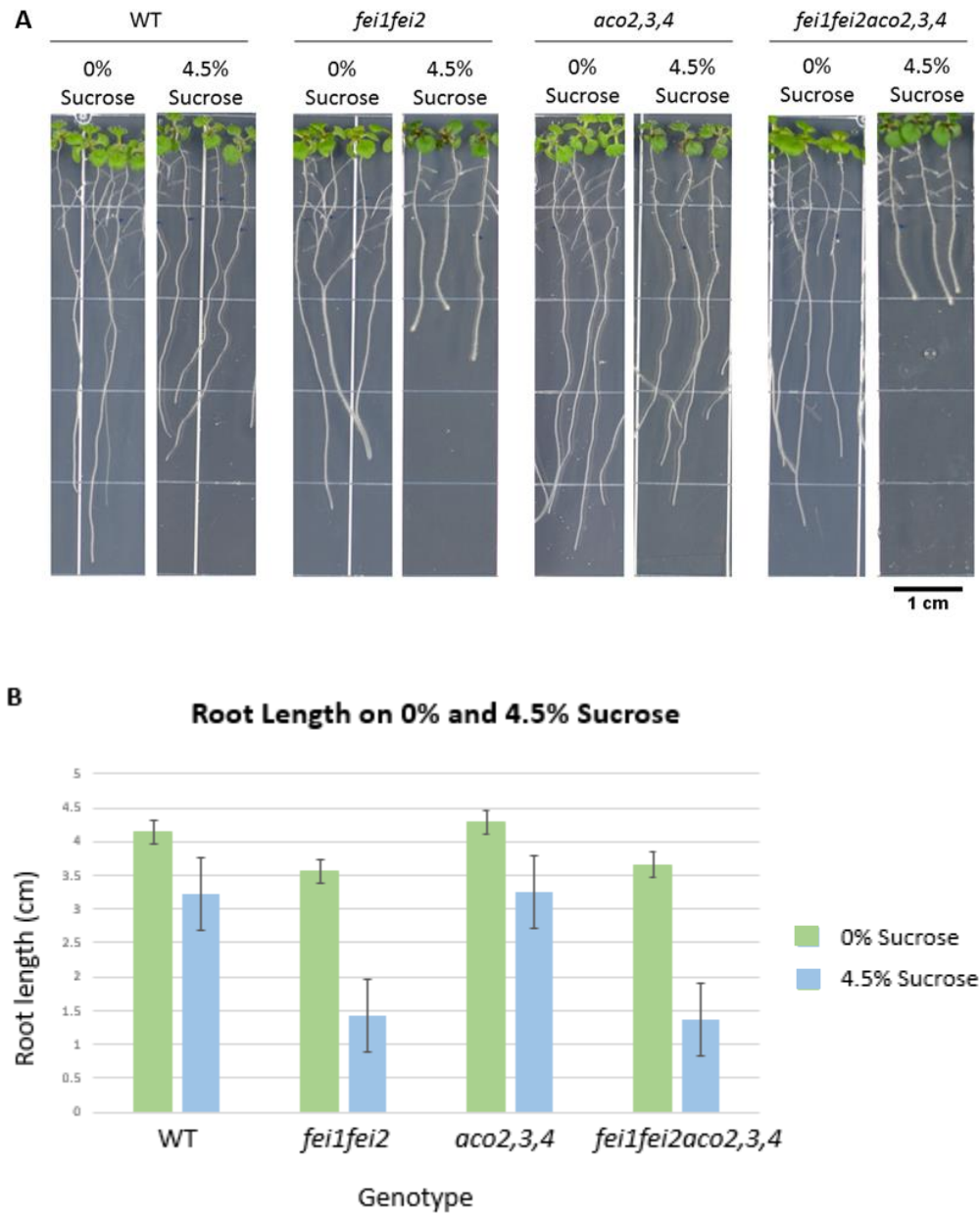


Figure 6. *aco2,3,4fei1fei2* root swelling is not enhanced compared to *fei1fei2*. **A.** Root length was imaged after four days on experimental media. **B.** Quantification of root length shows *aco2,3,4fei1fei2* is not shorter than *fei1fei2* (Student's t-test, $\alpha=0.05$).

Creating the multiple *aco* and *acs* mutants using CRISPR-Cas9

The CRISPR-Cas9 (Clustered Regularly Interspaced Short Palindromic Repeats) bacterial defense system has been adapted for the purposes of gene editing in model organisms

such as *Arabidopsis*, *Saccharomyces*, and *Xenopus* (Sander 2014). A guide RNA (gRNA) of 20 nucleotides targets the desired gene, and when a complementary sequence to the gRNA is found, the Cas9 enzyme cleaves the DNA. During non-homologous end joining (NHEJ), small insertions or deletions may occur during the repair process, creating a mutation in the targeted gene (Li et al. 2013). My previous attempts to create a septuple T-DNA type-2 *acs* mutant genes were not successful, possibly due to chromosomal rearrangements in the T-DNA mutants. Therefore, we designed CRISPR constructs to target the type-1, 2, and 3 *ACS* genes in the *feilfei2* and wt background. Two constructs, *acs4-1,5-1,8-1,9-1,11-1* (LR 20) and *acs4-2,5-2,8-2,9-2,11-2* (LR 21) will target the type-2 *ACS* genes. *ACS2-1,6-1,7-1* (LR23) and *ACS2-2,6-2,7-2* (LR22) will target the type-1 and -3 *ACS* genes. A CRISPR construct to target *ACO1,2,3,4,5* (LR24) was also synthesized, as root swelling phenotype of the *feilfei2 aco2,3,4* mutant line did not differ from *feil fei2* (**Fig. 6**). I will test if targeting all five *ACO* genes results in an enhanced root swelling phenotype.

Wild-type and *feilfei2* backgrounds were transformed using GATEWAY cloning and screened for editing through the T2 generation using Polyacrylamide Gel Electrophoresis (PAGE) (**Fig. 7**). Primers that flank the CRISPR recognition sequences were used to genotype plants to screen for CRISPR-Cas9 editing (**Table 1, Table 2**). In the T2 generation of LR20 (*ACS4,5,8,9,11-1*), editing was seen in *ACS4*, *ACS5*, and *ACS11* in the wild-type background, and in *ACS4* and *ACS5* in the *feilfei2* background. For LR21 (*ACS4,5,8,9,11-2*) T2s, sequencing confirmed that both LR21-14-10 and LR21-10-1 are double homozygous *acs4,9* mutants, and editing was seen on the PAGE gels for *ACS11* in the wild-type background. Additionally, in the *feilfei2* background, editing was seen for *ACS4*, *ACS5*, and *ACS11*. Editing was not seen for *ACS8* in the wild-type or *fei* background in LR20 or LR21 transformants on PAGE gels. In LR22

(*ACS2,6,7-2*) and LR23 (*ACS2,6,7-1*) editing was seen for all three genes in individual plants. For LR24 (*ACO1,2,3,4,5*), editing was seen in all genes in individual wild-type background plants, and for *ACO2,3,4,5* in the *feilfei2* background. In LR22, LR23, and LR24, editing was only seen in individual plants, so crosses will need to be done in the future to create the homozygous triple and quintuple mutants. However, the editing in individual plants of the same background indicates that the constructs are functional and editing may occur in future generations. Additionally, CRISPR editing may not have occurred uniformly in the plant, but heteroduplex formation is indicative of editing events (**Fig. 7**). Heteroduplex formation can occur when a mutated DNA strand forms a dimer with the wild-type strand. Because the base pair mismatches create an open angle between the two strands of DNA, a heteroduplex will run much slower on the gel than a perfect duplex of DNA strands (Zhu et al. 2014). These editing events may not persist through the germline, thus future generations have been selected based on the preliminary screening for stable mutations.

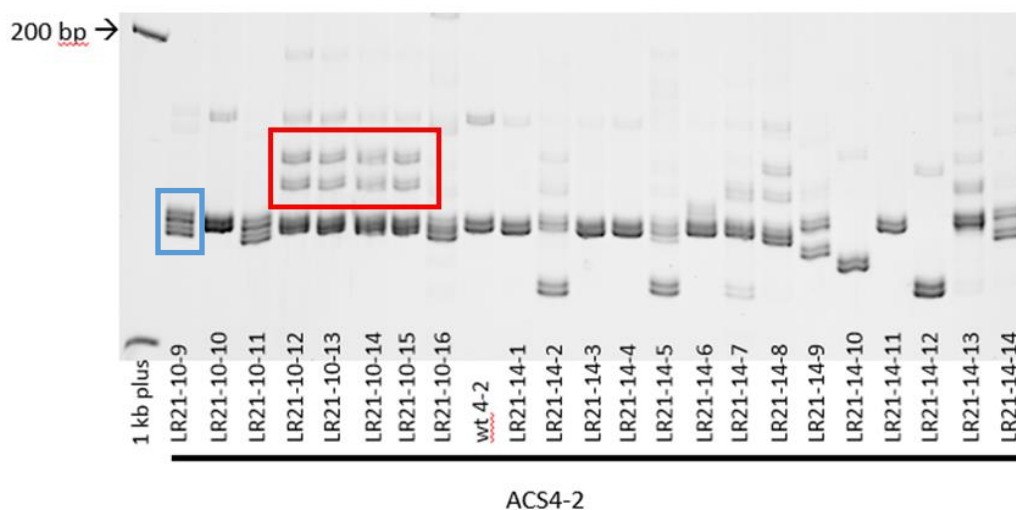
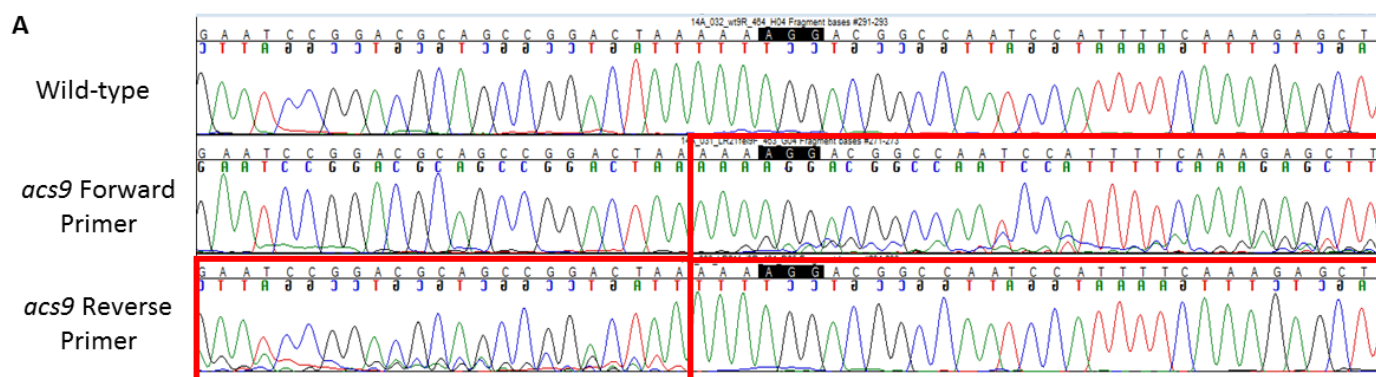


Figure 7. An example of a polyacrylamide gel electrophoresis used to screen for CRISPR-induced editing. LR numbers indicate the transformation event followed by the selected seedling number and seedling progeny number. The red box denotes examples of heteroduplexes, while the blue box highlights an example of a heterozygous sample.

In *Arabidopsis*, double stranded break repair most commonly results in single base pair insertions or small deletions (Feng et al. 2014). Because polyacrylamide gels are not high-resolution enough to robustly show one base-pair differences, derived Cleaved Amplified Polymorphic Sequences (dCAPS) primers were designed around the expected editing site for the target sites. dCAPS primers introduce a restriction enzyme site to the wild-type DNA, allowing for restriction enzyme analysis. These restriction enzyme sites are disrupted by the small insertions or deletions that result from CRISPR editing, so that the restriction enzymes can no longer cleave the DNA. Previously, DNA samples were bulked and sequenced for editing. If editing is occurring in the plant, there is a distinct pattern in the chromatogram (**Fig 8A**). dCAPS primers were tested on samples that showed editing on PAGE gels and through sequencing to determine if CRISPR events would disrupt the restriction site successfully. dCAPS analysis for *ACS5* show that CRISPR editing disrupted the XcmI dCAPS site for LR20-30-5 (*ACS4,5,8,9,11-1*) (**Fig. 8B**). dCAPS PCR and restriction enzyme conditions are being optimized to effectively genotype future generations selected from the earlier PAGE and sequencing results.



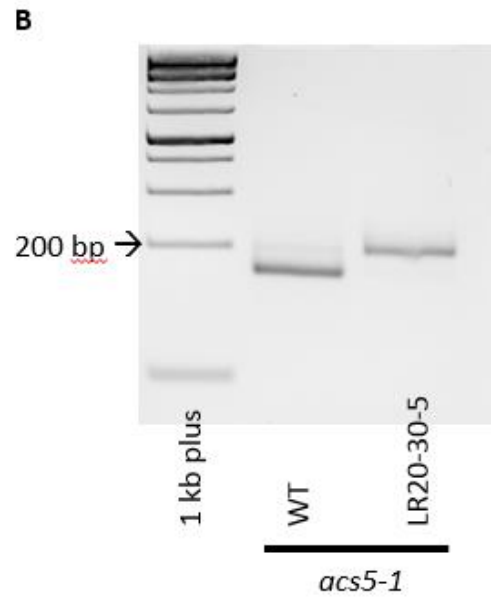


Figure 8. Location of editing allows for the use of dCAPS as a screening method. **A.** Chromatograms show a distinct pattern of CRISPR editing in the ACS9 gene. Editing occurs three base-pairs from the PAM (highlighted in black). **B.** dCAPS primers introduce a restriction enzyme site that overlaps with the region of CRISPR editing. Editing will disrupt the restriction site and prevent the enzyme from cutting the DNA, such as in LR20-30-5. Expected cut size for the wild-type is 166 bp, and the expected uncut size is 196 bp.

Discussion

Further experiments performed on AIB grown seedlings to determine if exogenous ACC could restore the root swelling phenotype of *feilfei2* showed the swelling was restored when seedlings were grown on AIB and ACC. This indicates that ACC could be acting as a signaling molecule. An ethylene insensitive *feilfei2ein2-5* mutant was used to confirm that the root morphology was not due to root responses mediated by ethylene (**Fig. 4**). These results will be confirmed using the *feilfei2acs4,5,8,9,11* mutant, as the high levels of inhibitors may have secondary effects that confound the interpretation of the results. Interestingly, the strong ethylene insensitive line, *ein2-5*, displayed a shortened root response to ACC application but not to

ethylene. This further supports the hypothesis that ACC has an additional function outside of ethylene biosynthesis.

To clarify the role of ACC as a signaling molecule outside of its function in ethylene biosynthesis, I aim to create several mutant lines that affect endogenous ACC levels using CRISPR-Cas9 technology. CRISPR sequences were designed to target *ACS4,5,8,9,11*, *ACS2,6,7*, and *ACO,2,3,4,5* to create null mutant lines. A double *acs4,9* mutant has been confirmed through sequencing, and heterozygotes for *acs5* have been isolated on PAGE gels. Based on PAGE analysis, CRISPR targeting *ACS8*, in both wt and *feilfei2* plants, did not result in editing events. Possibly, the gels were not high-resolution enough for single-base pair mutations to be detected. Alternatively, the CRISPR recognition sequence may not be effective for the target gene. CRISPR recognition sequences may not function *in vivo* for reasons such as chromatin modifications that block Cas9 activity, although the sequences may meet all known requirements *in silico*, such as being 20 nucleotides long and adjacent to a Protospacer Adjacent Motif (PAM). Because editing was not seen in certain genes on the PAGE gels, DNA samples were pooled for multiple lines and sequenced to screen for underlying editing events. A distinct pattern occurs three base-pairs from the PAM, where Cas9 is known to cut. The trace is distinct for each base until the site of editing is reached, and then the background trace will become disorganized, with multiple peaks (**Fig. 8A**). Editing was seen in the traces in the wild-type or *feilfei2* background for *acs4*, *acs5*, *acs9*, and *acs11* but not *acs8*. An *acs8* T-DNA line has been genotyped to cross to the CRISPR lines, as the *ACS8* CRISPR recognition sequences appear to be dysfunctional. Additionally, sequencing revealed editing not seen on PAGE gels, indicating that the PAGE gels do not accurately reflect the genotype of the plant. Because double strand break repair in *Arabidopsis* frequently results in one base-pair indel mutations, dCAPS primers have been

designed to screen for these small mutations. Small insertions or deletions will disrupt the dCAPS site, so a restriction enzyme will not cut DNA sequences with CRISPR editing events. These primers have been tested on known editing events seen on PAGE gels that were confirmed by sequencing (**Fig. 8B**). T3 progeny of each LR construct will be grown and screened using dCAPS primers and restriction enzyme analysis.

Tsuchisaka et al. 2009 found that an octuple *acs2,4,5,6,7,9,amiR8,11* mutant was embryonic lethal. Because artificial microRNA used in that study may not be completely effective at suppressing gene expression and chromosomal rearrangements from T-DNA insertions can result in lethality, I am creating an octuple *acs2,4,5,6,7,8,9,11* mutant using CRISPR/Cas9 to confirm the effects of an octuple *acs* mutant. To do so, I have crossed plants containing the CRISPR constructs LR21 (*acs4-2,5-2,8-2,9-2,11-2*) and LR23 (*acs2-2,6-2,7-2*). The progeny of these crosses have been grown and will be screened for editing using dCAPS primers and restriction enzyme analysis.

Once the lines are obtained, the *feilfei2acs4,5,8,9,11* plants will be grown on high sucrose media to determine if the swollen root phenotype is rescued to a wild-type morphology. ACC levels should be reduced, as low levels of ACS activity will inhibit the conversion of AdoMet to ACC. Similarly to inhibiting ACC via application of AIB, low ACC levels may result in a reversion of the *feilfei2* phenotype. If the *fei* phenotype is reverted in this line, we then aim to see if applying ACC exogenously will restore the swelling. Additionally, the octuple *acs2,4,5,6,7,8,9,11* mutant will be characterized for phenotypes such as lethality to confirm the previous findings using artificial microRNA and T-DNA insertions (Tsuchisaka et al. 2009). The *feilfei2aco1,2,3,4,5* line will be grown on high and low sucrose to determine if an enhancement of the *fei* phenotype occurs. Because the activity of the ACC oxidases will be limited, ACC

should not be converted to ethylene, leading to elevated levels of ACC within the plant. We hypothesize that this increase in ACC will lead to an enhancement of the *fei* phenotype, such as increased swelling and a decrease in root elongation. Previous experiments using a *fei1fei2aco2,3,4* T-DNA line did not show any difference in morphology compared to the *fei1fei2* phenotype, and we aim to see if creating mutations in the remaining *ACO* genes will result in a stronger phenotype. Taken together, these results will further illuminate the novel role of ACC in the FEI pathway.

Materials and Methods

Plant Growth

Seeds were washed with 95% ethanol, incubated in a bleach solution [50% bleach, 0.1% tween-20 (Fisher Scientific)] and washed with sterile deionized water at least three times. Seeds were then plated on media using a pipette tip to pick up seeds and deposit them onto the media. For selection of plants with the CRISPR-Cas9 vector, seeds were grown on an MS media consisting of phytigel (Sigma Lifescience) at 6g/L and MS salts (Research Products International) at 4.8g/L, pH 5.6, 1% sucrose, and 50 µg/ml BASTA (Gold Biotechnology). Seeds were stratified for four days in 4°C, and grown in light in 22°C until resistant seedlings could be differentiated. Seedlings were transferred to soil and grown in 24 hour light cycle. Seeds were harvested using a mesh filter and stored in envelopes at room temperature. For various physiological root assays, seeds were grown on an MS media consisting of phytigel (Sigma Lifescience) at 6 g/L and MS salts (Research Products International) at 4.8 g/L, pH 5.6, 0% sucrose, 10 µM ACC, 0.4 mM AIB, and/or 4.5% sucrose.

Genotyping procedure

CRISPR editing was determined by amplifying 60-80 base pairs around the target region using primers that flank the CRISPR target sites. PCR was performed and the PCR product was run at 90V on a 15% polyacrylamide gel {24.9 mL 29% 29.5:1 acrylamide:bis-acrylamide mixture (National Diagnostics), 19.75 mL H₂O, 5 mL 10x TBE, 350 µL 10% ammonium persulfate (Fisher Scientific), 17.5 µL N,N,N',N'-tetramethylethylenediamine (Sigma Life Science)}. Gels were stained with 0.5x TBE+0.05 µL/mL ethidium bromide (Fischer Scientific) solution for 45 minutes with gentle shaking and imaged with a ChemicDoc Touch Imaging System (Bio-Rad).

Root Elongation and Swelling Assay

To test the effects of ACC and ethylene, seedlings were transferred at four days from MS-MES plates to media with 1 mM AIB, 10 µM ACC, or flushed with ethylene gas (10 ppm). Roots were imaged using a Leica MZ FL III fluorescence stereomicroscope and plates were scanned using an Epson scanner. Root length was measured after seven days using ImageJ (Abramoff 2004).

Derived Cleaved Amplified Polymorphic Sequence (dCAPS) and Cleaved Amplified Polymorphic Sequence (CAPS)

dCAPS sites were designed using the New England Biolabs “Alphabetized List of Recognition Specificities” and the wild-type sequences for each gene on the *Arabidopsis* website. PCR was performed using primers in **Table 2**. PCR products were digested with specific restriction enzymes under the conditions listed in **Table 3**.

Table 1. Forward (F) and Reverse (R) Primers Flanking CRISPR target sites in **Table 2** for *ACS2,4,5,6,7,8,9,11* and *ACO1,2,3,4,5*

Target Gene	Primer Name	Sequence
<i>ACS4-1</i>	crACS4-1F_60bp	AAGAGTACGAGAAGAATCCT
	crACS4-1R_60bp	CCATCTGGATAATGCCTTGA
<i>ACS5-1</i>	crACS5-1F_60bp	TATGATGAGATCAAGAACCC
	crACS5-1R_60bp	TAGCTGGTTTTTCGGCTAGAC
<i>ACS8-1</i>	crACS8-1F_60bp	CCTTACGACGAGATCAAGAA
	crACS8-1R_60bp	CTGATTTTCTGCTAGACCCA
<i>ACS9-1</i>	crACS9-1F_60bp	CCTTACGACGAAATCAAGAA
	crACS9-1R_60bp	CTGATTTTTCGGCAAGACCCA
<i>ACS11-1</i>	crACS11-1F_60bp	TCCGTTCTTTTTGCAGCTTT
	crACS11-1R_60bp	TCTGGATGCTCTTCAAGCCA
<i>ACS4-2</i>	crACS4-2F_60bp	TATTGGATTTCTGTAGCTAT
	crACS4-2R_60bp	TCTGTGTTTTGTGCAAGCCA
<i>ACS5-2</i>	crACS5-2F_60bp	GATCCAGATGGGTCTAGCCG
	crACS5-2R_60bp	GTAAACCATGACTCGATTAG
<i>ACS8-2</i>	crACS8-2F_60bp	ATGGCTTGCTAAGAACCCCG
	crACS8-2R_60bp	CGAAATATGGATTGGCCTTC
<i>ACS9-2</i>	crACS9-2F_60bp	ACATGGTTAGCTAAGAATCC
	crACS9-2R_60bp	GAAAATGGATTGGCCGTCCT
<i>ACS11-2</i>	crACS11-2F_60bp	GCTCTGTTCCAAGATTACCA
	crACS11-2R_60bp	TCCAATATGTTACTTACAT
<i>ACS2-1</i>	crACS2-1F_60bp	CTTTTCATCTTTCCCGTAAC
	crACS2-1R_60bp	CCTGATTCTCTGCAAGACCC
<i>ACS6-1</i>	crACS6-1F_60bp	TCTATTGTCTAAAATCGCCT
	crACS6-1R_60bp	CCATCGAAATAAGAGGAATT
<i>ACS7-1</i>	crACS7-1F_60bp	ACTTGGAGAAGAAGAATCCA
	crACS7-1R_60bp	GGAACCCAGGAGCTCCTTTT
<i>ACS2-2</i>	crACS2-2F_60bp	AGCGACATCGCTAATTTCCA
	crACS2-2R_60bp	TTATAGTACCTGTCTAAACT
<i>ACS6-2</i>	crACS6-2F_60bp	TTTCTGAATTGTGTAGCTTT
	crACS6-2R_60bp	TCTGGATGTTTTAAAACCCA
<i>ACS7-2</i>	crACS7-2F_60bp	GGGGATCAAAGGAGCTCCT
	crACS7-2R_60bp	GACCGTGGTAGTCTTGAAC
<i>ACO1</i>	crACO1F_60bp	TCACTTCTTGATCATGCATG
	crACO1R_60bp	TAAAGATGTTATACATACCA
<i>ACO2</i>	crACO2F_60bp	AATGGGGAAGAGAGAGACCA
	crACO2R_60bp	GCCCCAATTCTCACAAGCTT
<i>ACO3</i>	crACO3F_60bp	GACCAAACCATGGCTTTGAT
	crACO3R_60bp	AAGAACCTCGAAGAAGCCCC
<i>ACO4</i>	crACO4F_60bp	AGCAATCACTATGGAGAAGA
	crACO4R_60bp	AGTACCTCAAAGAAGCCCCA

<i>ACO5</i>	crACO5F_60bp	AGAGAAGACACTGTCTGAAA
	crACO5R_60bp	CGAACCTGAAAAAATCCCCA

Table 2. CRISPR Design to Target *ACS2,4,5,6,7,8,9,11* and *ACO1,2,3,4,5* Genes

CRISPR Construct	Target Gene (AT number)	Recognition Sequence
<i>crACS2-1</i>	<i>ACS2</i> (AT1G01480)	CCCCATGGGATCATCCAAAT
<i>crACS2-2</i>	<i>ACS2</i> (AT1G01480)	AGACTACCATGGTCTTAAGA
<i>crACS4-1</i>	<i>ACS4</i> (AT2G22810)	TACGACGTTACCAAGAACCC
<i>crACS4-2</i>	<i>ACS4</i> (AT2G22810)	GCTTTGATCTACTAGAGTCA
<i>crACS5-1</i>	<i>ACS5</i> (AT5G65800)	TAATGGGATGATCCAGATGG
<i>crACS5-2</i>	<i>ACS5</i> (AT5G65800)	AAAACCAGCTATGTTTCGAT
<i>crACS6-1</i>	<i>ACS6</i> (AT4G11280)	CCGGTGACGGTCACGGCGAG
<i>crACS6-2</i>	<i>ACS6</i> (AT4G11280)	GTGGAGATTTGATGCGTAAA
<i>crACS7-1</i>	<i>ACS7</i> (AT4G26200)	GAAGGTTTCGATGTGGGGATC
<i>crACS7-2</i>	<i>ACS7</i> (AT2G26200)	GGGTTCCGTGAAAACGCATT
<i>crACS8-1</i>	<i>ACS8</i> (AT4G37770)	CCCAGACGGCATTATCCAAA
<i>crACS8-2</i>	<i>ACS8</i> (AT4G37770)	ACGCAGCCAATTTCCAAAGA
<i>crACS9-1</i>	<i>ACS9</i> (AT3G49700)	CCCTAATGGGATTATTCAAAA
<i>crACS9-2</i>	<i>ACS9</i> (AT3G49700)	GGACGCAGCCGGACTAAAAA
<i>crACS11-1</i>	<i>ACS11</i> (AT4G08040)	CTTTTGACCTAATAGAGAAA
<i>crACS11-2</i>	<i>ACS11</i> (AT4G08040)	TGGCTTGCCAGCTTTCAAGG
<i>crACO1-1</i>	<i>ACO1</i> (AT2G19590)	TGATAAGTGGGGATTCTTCA
<i>crACO2-1</i>	<i>ACO2</i> (AT1G62380)	CATTGATTAGAGCCATGGTT
<i>crACO3-1</i>	<i>ACO3</i> (AT1G12010)	CGACGATGCTTGTCAAAACT
<i>crACO4-1</i>	<i>ACO4</i> (AT1G05010)	TCAAAGACGCTTGTGAAAAC
<i>crACO5-1</i>	<i>ACO5</i> (AT1G77330)	TCGCTAGAGCTTGCGAAGAG

Table 3. dCAPS primer sequences used to introduce a restriction enzyme (RE) site to wild-type.

Target site	Primer Name	Primer	RE
<i>ACS4-1</i>	dCAPS_ACS4-1F_BsII	TACATGCAACAGCCATGGCCAAGTCTCTTCGTATTTACTT	BsII
	dCAPS_ACS4-1R_BsII	TGGATAATGCCTTGAGGGTCTTGGTACCGT	
<i>ACS4-2</i>	392 crACS4-2F	CAGAGAGACTAATTTAAAGT	HinfI
	CAPs_ACS4-2Rev	GTTCCCGGAAAACAGACTGG	
<i>ACS5-1</i>	dCAPS_ACS5-1Fwd	AGAAGAATCCTTATGATGAGATCCAGAACC	XcmI
	dCAPS_ACS5-1Rev	TTGAATTCAGGCATGCCATG	
<i>ACS5-2</i>	dCAPS_ACS5-2Fwd	GACAAGCAATGGTCATGGAC	BsII
	dCAPs_ACS5-2Rev	CATGACTCGATTAGATCGAAACATAGCCGG	
<i>ACS8-1</i>	dCAPS_ACS8-1Fwd	ACGACGAGATCAAGAACCCAGACGCCATTA	XcmI
	crACS8-2R_60bp	CGAAATATGGATTGGCCTTC	

<i>ACS8-2</i>	dCAPS_ACS8-2Fwd	TTGAGTCATGGCTTGCTAAGAACGCCGAC	MwoI
	dCAPS_ACS8-2Rev	GGTTACGTTGTCATATCGTT	
<i>ACS9-1</i>	dCAPS_ACS9-1Fwd	CGACGAAATCAAGAACCCTAATGCCATTAT	XcmI
	crACS9-2R_60bp	GAAAATGGATTGGCCGTCCT	
<i>ACS9-2</i>	dCAPS_ACS9-2Fwd	TTAGCTAAGAATCCGGACGCAGCCGGCCTA	BsII
	ACS9seqR	CTTGCTTGATCAAATGTTA	
<i>ACS11-1</i>	dCAPS_ACS11-1Fwd	TTCTTTTGCAGCTTTCTTTTGACCCAATA	XcmI
	dCAPS_ACS11-1Rev	CTTACATCCTTGAAAGCTGGCAAGCAATGG	
<i>ACS11-2</i>	406 crACS11-1F	GTACACAATTTCCAAACTTT	Bsli
	dCAPS_ACS11-2Rev	ATATGTTACTTACATCCTTGAAAGCTGCCAA	
<i>ACS2-1</i>	dCAPS_ACS2-1Fwd	CATCTTTCCCGTAACCCCATGCCATCATC	XcmI
	dCAPS_ACS2-1Rev	TAGCTTGATGTGTATACGTG	
<i>ACS2-2</i>	CAPS_ACS2-2Fwd	GAACCCAGAAGCTTCTATTT	XcmI
	413 crACS2-2R	GTAGCTGATTACAAGATATC	
<i>ACS6-1</i>	dCAPS_ACS6-1_AleI	GATCTGAATCTATTGTCTAAAATCCACTCC	AleI
	CAPs_ACS6-1Rev	TGATTTTCAGCGAGACCCAT	
<i>ACS6-2</i>	dCAPS_ACS6-2Fwd	GAAGAAAACCCATTTACCC	MwoI
	dCAPS_ACS6-2Rev	ATCGAAGCTTCTGGATGTTTTAAAAGCCAT	
<i>ACS7-1</i>	dCAPS_ACS7-1F_XcmI	GAAACTTACTTGGAGAAGAAGAATCCACCA	XcmI
	dCAPS_ACS7-1R_XcmI	AGTTCGTTAGCGCGGTGGC	
<i>ACS7-2</i>	418 crACS7-1F	CAAACAGGTCTCGTTTGATC	BsII
	dCAPS_ACS7-2Rev	GGTAGTCTTGAAACAATGCGTTTTACCGA	

Table 4. Restriction enzyme digest parameters for dCAPS analysis.

Enzyme	Buffer	Incubation Temp (°C)	Incubation Time (hr)	Heat Inactivation Temp (°C)	Heat Inactivation Time (min)
XcmI	NEB2.1	37	2	65	20
HPY99I	Cutsmart	37	1	65	20
MwoI	Cutsmart	60	1	no	no
BsII	Cutsmart	55	1	no	no
HinfI	Cutsmart	37	1	80	20
BstXI	NEB3.1	37	1	80	20
BsaWI	Cutsmart	60	1	80	20

Acknowledgments

Thank you, Joanna Polko, for mentoring me throughout my research experience in the Kieber lab. Many thanks also to Joseph Kieber, Christian Burr, Carly Shanks, Charles Hodgens, Nicole

Chang, Katy Citrin, and Amy Maddox for their feedback and guidance on preparing this manuscript and presentation. Lastly, thank you Ian Street and Eric Schaller for your work with the *ein2-5* mutants.

References

- Abramoff MD, Magelhaes PJ, Ram SJ (2004) Image Processing with ImageJ. *Biophotonics International*, 11: 36–42.
- Alonso, J.M., Stepanova, A.N., Leisse, T.J., Kim, C.J., Chen, H., Shinn, P., Stevenson, D.K., Zimmerman, J., Barajas, P., Cheuk, R., Gadrinab, C., Heller, C., Jeske, A., Koesema, E., Meyers, C.C., Parker, H., Prednis, L., Ansari, Y., Choy, N., Deen, H., Geralt, M., Hazari, N., Horn, E., Karnes, M., Mulholland, C., Ndubaku, R., Schmidt, I., Guzman, P., Aguilar-Henonin, L., Schmid, M., Weigel, D., Carter, D.E., Marchand, T., Resseeuw, E., Brogden, D., Zeko, A., Crosby, W.L., Berry, C.C., Ecker, J.R. (2003) Genome-Wide Insertional Mutagenesis of *Arabidopsis thaliana*. *Science*, 301: 653-657.
- Aeschbacher R., Hauser M.-T., Feldmann K.A., Benfey P.N. (1995). The *SABRE* Gene is Required for Normal Cell Expansion in *Arabidopsis*. *Genes Dev.*, 9: 330-340
- Arioli T., Peng L., Betzner A.S., Burn J., Wittke W., Herth W., Camilleri C., Hofte H., Plazinski J., Birch R., Cork A., Glover J., Redmond J., Williamson R.E. (1998). Molecular Analysis of Cellulose Biosynthesis in *Arabidopsis*. *Science*, 279(5351):717-720.
- Feng, Z., Mao, Y., Xu, N., Zhang, B., Wei, Pengliang., Yang, D-L., Wang, Z., Zhang, Z., Zheng, R., Yang, L., Zeng, L., Liu, X., Zhu, J-K. (2014). Multigeneration Analysis Reveals the Inheritance, Specificity, and Patterns of CRISPR/Cas-induced Gene Modifications in *Arabidopsis*. *Proc. Natl. Acad. Sci.*, 111(12): 4632-4637.
- Givens C. (2010). A Physiological and Evolutionary Study of the Plant Hormone Ethylene (Ph.D. Dissertation). The College of William and Mary.
- Guzman, P., Ecker, J.R. (1990). Exploiting the Triple Response of *Arabidopsis* to Identify Ethylene-Related Mutants. *The Plant Cell*, 2:513-523.
- Ju C., Yoon G.M., Shemanksy J.M., Lin D.Y., Ying Z.I., Chang J., Garrett W.M., Kessenbrock M., Groth G., Tucker M.L., Cooper B., Kieber J.J., Chang C. (2012). CTR1 Phosphorylates the Central Regulator EIN2 to Control Ethylene Hormone Signaling from the ER Membrane to the Nucleus in *Arabidopsis*. *Proc. Natl. Acad. Sci. U.S.A.*, 109(47): 19486-19491.
- Li J., Norville J.E., Aach J., McCormack M., Zhang D., Bush J., Church G.M., Sheen J. (2013). Multiplex and Homologous Recombination-Mediated Genome Editing in *Arabidopsis* and *Nicotiana benthamiana* Using Guide RNA and Cas9. *Nature Biotechnology*, 31(8): 688-691.
- Li, W., Ma, M., Feng, Y., Li, H., Wang, Y., Ma, Y., Li, M., An, F., Guo, H. (2015). EIN2-Directed Translational Regulation of Ethylene Signaling in *Arabidopsis* Article EIN2-Directed Translational Regulation of Ethylene Signaling in *Arabidopsis*. *Cell*, 163(3): 670–683.
- Nacry, P., Camilleri, C., Courtial, B., Caboche, M., Bouchez, D. (1998). Major Chromosomal Rearrangements Induced by T-DNA Transformation in *Arabidopsis*. *Genetics*, 149(2): 641-650.

Sander J.D., Joung J.K. (2014). CRISPR-Cas Systems for Editing, Regulating, and Targeting Genomes. *Nature Biotechnology*, 32(4): 347-355.

Tsang D.L., Edmond C., Harrington J.L., Nühse T.S. (2011). Cell Wall Integrity Controls Root Elongation via a General 1-aminocyclopropane-1-carboxylic acid-Dependent, Ethylene-Independent Pathway. *Plant Physiology*, 156: 596-604.

Tsuchisaka A., Yu G., Jin H., Alonso J.M., Ecker J.R., Zhang X., Gao S., Theologis A. (2009). A combinatorial interplay among the 1-aminocyclopropane-1-carboxylate isoforms regulates ethylene biosynthesis in *Arabidopsis thaliana*. *Genetics*, 183: 979-1003.

Wang, K.L-C., Li, H., Ecker, J.R. (2002). Ethylene Biosynthesis and Signaling Networks. *The Plant Cell*, S131-S151.

Wolf, S., Hematy, K., Hofte, H. (2012). Growth Control and Cell Wall Signaling in Plants. *Annu. Rev. Plant Biol.*, 63:381-407.

Xu S., Rahman A., Baskin T.I., Kieber J.J. (2008). Two Leucine-Rich Repeat Receptor Kinases Mediate Signaling, Linking Cell Wall Biosynthesis and ACC Synthase in *Arabidopsis*. *The Plant Cell*, 20: 3065-3079.

Zhu, X., Xu, Y., Yu, S., Lu, L., Ding, M., Cheng, J., Song, G., Gao, X., Yao, L., Fan, D., Meng, S., Zhang, X., Hu, S., Tian, Y. (2014) An Efficient Genotyping Method for Genome-modified Animals and Human Cells Generated with CRISPR/Cas9 System. *Nature Scientific Reports*, 4:6420.